Pergamon

0042-6989(94)00285-1

Vision Res. Vol. 35, No. 14, pp. 1965–1978, 1995

0042-6989/95 $9.50 + 0.00

Zero Frequency Masking and a Model of Contrast Sensitivity*

JIAN YANG,† XIAOFENG QI,† WALTER MAKOUS†‡

Received 14 January 1994; in revised form 22 September 1994; in final form 27 October 1994

Stimulating the visual system tends to desensitize it to certain stimulus properties. Such desensitization is usually called adaptation or masking, but the distinction between the two is unclear. Nonspecific desensitization by light is usually regarded as adaptation, whereas pattern-specific desensitization is typically considered masking. Here we unify the treatment of such desensitizing phenomena by handling both in the spatial frequency domain. The amount of adapting light in a stimulus is represented in the spatial frequency domain by the component at zero frequency. To determine whether such adapting light acts like other components in the spatial frequency domain, we compared the effect of masking by the zero frequency component with the effects of masking by components at other frequencies. We show that the zero frequency component acts like other masking components, decreasing sensitivity to nearby test frequencies and thereby producing the insensitivity to low spatial frequencies that gives the contrast sensitivity curve its band-pass shape at high light levels. Treating light adaptation as masking by the zero frequency component leads to a general model that describes visual sensitivity to test gratings of varying spatial frequency at varying mean luminance, in the presence (or absence) of masking gratings of varying spatial frequency. Individual components of the model provide insight into visual processing at the system level.

Grating Amplitude sensitivity Zero frequency component Luminance Masking Quantitative model

INTRODUCTION

Stimulating the visual system tends to desensitize it to certain properties of the stimulus. Such desensitization is often called either adaptation or masking. Although usage of the two terms tends to differ, the distinction between them is unclear. In any case, the phenomena are similar in that they both describe a loss of sensitivity exerted by one stimulus on other stimuli that resemble it in certain ways, and this similarity between the two phenomena raises the possibility of treating both within a uniform and consistent framework that focuses on their similarities instead of their differences. We have taken a step in that direction here by treating the desensitizing effects of the total amount of light in a stimulus, usually regarded as adaptation, in the same context as the desensitizing effects of the spatial modulation associated with gratings, usually regarded as masking. Specifically, the total light available for adaptation in any stimulus is represented by the Fourier component at zero spatial frequency (sometimes called the d.c. *component*, from usage that evolved in connection with electronic signals), and we treat the spread of adaptation in the Fourier domain instead of the spatial domain. When we do use the term masking, we mean to imply nothing by the term except a desensitization described in the spatial frequency domain instead of the spatial domain. Of course the two domains are related, and it should be possible to work entirely within the spatial domain instead. However, the approach used here has proven useful for understanding the spatiotemporal *in*separability of contrast sensitivity curves measured by counterphase modulation, as well as the spatiotemporal *separability* of contrast sensitivity curves measured by inphase modulation (Yang & Makous, 1994a). This approach also proves useful here and in allied work (Yang & Makous, 1995), for it leads to a model, founded on well established principles of visual function, that relates directly to fundamental properties of the visual system and economically describes visual sensitivity along 7 dimensions: i.e. sensitivity to test gratings of varying (1) spatial and (2) temporal frequency at varying (3) mean luminance, in the presence of masking gratings of varying (4) amplitude, (5) phase, (6) spatial and (7) temporal frequency.

*An early version of this paper was presented at the annual meeting of the Association for Research in Vision and Ophthalmology, in Sarasota, Fla, May 1992.

†Center for Visual Science, University of Rochester, Rochester, NY 14627, U.S.A.

‡To whom all correspondence should be addressed.

METHOD

Stimuli consisted of two horizontal sinusoidal gratings expressed by the formula:

$$s(x, y, t) = L^*[1 + C_m \sin(2\pi f_{Lm} y) + C_t \sin(2\pi\omega t)\sin(2\pi f_{Lt} y + \epsilon)], \quad (1)$$

where the luminance profile of the stimulus (s) is a function of space (x, y) and time (t), L^* is mean luminance, C_m is mask contrast, f_{Lm} is spatial frequency of the mask, C_t is test contrast, f_{Lt} is spatial frequency of the test grating, ω is the temporal frequency of the test grating, and ϵ takes random values from 0 to 2π to randomize the phase of the test grating relative to that of the mask. The stimulus, which was generated by a Pixar Image computer, extended over a 5.2 deg square on the center of a video screen, surrounded by a 10.4 by 13 deg field of uniform intensity equal to the mean luminance of the gratings, L^*. The video screen had 10-bit gray level resolution with linear gamma correction, and a maximum luminance of 50 cd/m^2. Observers viewed the stimulus binocularly, with a chin rest, in direct view without artificial pupils. The three authors, who all had normal corrected vision, served as the observers.

The psychophysical procedure was two alternative temporal forced choice, with random presentation of the test stimulus in one of the two intervals. Each temporal interval lasted 1 sec, with 0.4 sec between the two intervals. A fixation cross was displayed at all times except during the two intervals. Each interval was demarcated by a beep and absence of the fixation cross. The observers' task was to indicate which interval contained the test stimulus. Trials were initiated by the observer. The contrast of the test on each trial was determined by a procedure that searched for the contrast correctly identified on 84% of the trials (Watson & Pelli, 1983). Auditory signals informed the observer about the correctness of the preceding response. A given session, wherein the temporal frequency, mean luminance, mask contrast and mask spatial frequency were fixed, consisted of 300 trials of six different spatial frequencies, randomly interleaved.

The spatial contrast sensitivity curve was measured without a masking grating (i.e. a conventional contrast sensitivity curve without a mask) or with a masking grating, which was displayed continuously during a run at 0.1 contrast ($C_m = 0.1$) and at one of two spatial frequencies (f_{Lm}): 2 or 4 c/deg. The test frequencies for the conventional contrast sensitivity curve ranged from 0.5 to 16 c/deg, and those with a masking grating ranged from slightly higher than the mask frequency to 16 c/deg. Measurement of these three curves was repeated for each observer first at four different luminances, $L^* = 0.019$, 0.20, 2.1 and 42 (25 for WM) cd/m^2 with a temporal frequency of 0.5 Hz (i.e. the first half period of 0.5 Hz sine wave), then with the test grating modulated at a different temporal rate ($\omega = 4$ Hz) at the highest luminance. The results, averaged over four runs, are plotted as amplitudes (contrast times the mean luminance) instead of contrasts to simplify exposition; this, of course, does not alter the shapes of the individual curves.

MASKED SENSITIVITY

Results

As the shapes of the sensitivity curves from the three observers were similar, we have combined them to increase their smoothness and precision. Figure 1 shows the resulting mean sensitivities at the highest mean luminance (42 cd/m^2 for XQ and JY, and 25 for WM). The error bars represent the standard errors across observers.

Discussion

All three curves have the shape of typical band-pass filters. The differences among the curves, i.e. the reduced sensitivity to gratings of low frequency shown by the curves with open symbols relative to the curve with solid squares, is attributed to desensitization by the Fourier components of the masking gratings. The curve with solid squares is usually taken to represent pure detection sensitivity without masking, but this depends on the assumption, seldom explicit, that the zero frequency component of test gratings does not cause masking. However, this curve (with solid squares) shows reduced sensitivity to gratings near the Fourier component of the grating at 0 c/deg, relative to those of high frequency, that is both logically analogous and qualitatively similar to that near the 2 and 4 c/deg components. There is no basis, in this experiment at least, for treating these components differently, and the sensitivity losses are similar enough to raise the question whether the phenomena and mechanisms are similar.

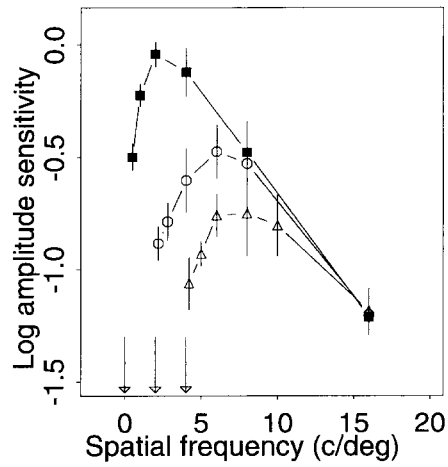

FIGURE 1. Amplitude sensitivities in td^{-1}, averaged over three observers, at mean luminances of 25 cd/m^2 for WM, and of 42 cd/m^2 for XQ and JY. The error bars represent the standard errors over three observers. The data points show the detection sensitivity (■), the masked sensitivity curves with mask spatial frequency at 2 (○) and 4 (△) c/deg, respectively. The arrows point to the mask frequencies, including zero as a masking frequency. The test gratings were counterphase modulated at 0.5 Hz.

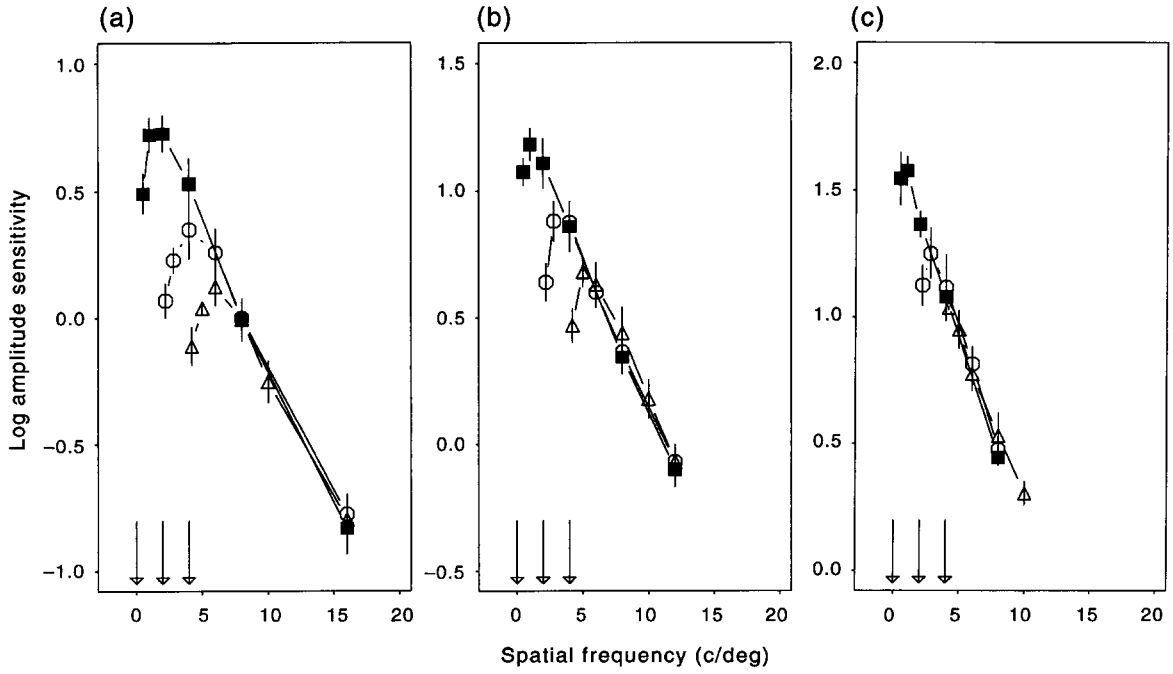

FIGURE 2. Amplitude sensitivities in td^{-1} with mean luminance of 2.1 (a), 0.20 (b), and 0.019 (c) cd/m^2, averaged over three observers. The data points show the detection sensitivity (■), the masked sensitivity curves with mask spatial frequency at 2 (○) and 4 (△) c/deg, respectively. The arrows point to the mask frequencies, including zero as a masking frequency. The test gratings were counter-phase modulated at 0.5 Hz.

If the mechanisms are similar, things that affect one ought to have similar effects on the other. Similarity of effects in the two cases does not prove that the mechanisms are the same, but if enough similarities accrue without exceptions, for most purposes the two can be treated as the same. Consequently, the following experiments were designed to determine whether experimental manipulations that reduce the sensitivity losses near zero frequency, namely reduced mean luminance and increased temporal frequency of the test grating, produce similar reductions near explicitly masked frequencies.

LUMINANCE

Methods

In this experiment, the mean luminance of the grating was reduced in roughly log unit steps from previous settings to 2.1, 0.20 and 0.019 cd/m^2. The luminances were decreased by having the observers wear goggles with opaque frames and neutral density filters over the transparent lenses. The temporal frequency of the test was again 0.5 Hz.

Results

The results among the three observers were again similar, and so we again show the mean results in Fig. 2. The three panels show the results at the three different luminances, decreasing from left to right. The solid squares are with no mask, the open circles with the 2 c/deg mask, and the open triangles with the 4 c/deg mask.

The results shown by the solid squares in Figs 1 and 2 show that reducing the mean luminance greatly reduced the attenuation of lower frequencies relative to the peak sensitivity for the corresponding curve. In other words, the sensitivity curve tended towards low-pass as mean luminance decreased, in agreement with many previous reports (e.g. Van Nes & Bouman, 1967; De Valois, Morgan & Snodderly, 1974). As in Fig. 1, this attenuation of lower frequencies can be explained by an effect analogous to masking; therefore, a low pass shape reflects little such masking, and reducing mean luminance reduces any such masking.

Reducing the mean luminance also greatly reduced the amount of masking, as shown by the curves with open symbols; i.e. the differences between the curves composed of open symbols and those composed of solid symbols are due to masking, and these differences decrease and almost disappear as mean luminance decreases. Decreasing the mean luminance of a masking grating of constant contrast decreases the amplitude of the masking component.

Therefore, these results show that reducing the amplitude of a masking component reduces the desensitization of nearby frequencies; analogously, reducing the amplitude of the component at 0 frequency also reduces the desensitization of nearby frequencies. This increases the similarity of the two kinds of desensitization, strengthening the idea that the low sensitivity at the low end of contrast sensitivity curves is similar to the low sensitivity near the frequency of a masking component.

TEMPORAL FREQUENCY

Methods

In this experiment, we increased the temporal frequency of the test grating from 0.5 to 4 Hz and returned to the luminances of the first experiment (42 cd/m^2 for XQ and JY, and 25 for WM). The contrast of the mask was still 0.1.

Results

Figure 3 shows the resulting contrast sensitivity functions. The attenuation of low spatial frequencies in the curve with no masking grating (solid squares), in these results with 4 Hz modulation of the test grating, is greatly reduced from that observed with 0.5 Hz modulation (Fig. 1, solid squares). This agrees with many previous studies (e.g. Robson, 1966; Kulikowski, 1971; Kelly, 1972). It is noteworthy that the effects of masking in these results with 4 Hz modulation (Fig. 3, open symbols) is also greatly reduced from that observed with 0.5 Hz modulation (Fig. 1, open symbols).

Discussion

Although the attenuation of low frequencies and the attenuation due to masking appear to behave similarly in the ways tested so far, it would be desirable to have a quantitative assessment of the similarity, as opposed to the present qualitative one. If the two depend quantitatively in the same ways on the same variables, the strength of similarity is increased. Consequently, we have derived the model described below to assess the dependence of these two phenomena on the experimental parameters quantitatively, but the model is useful in other ways as well.

A MODEL

Rationale

This model depends on representation of stimuli in the spatial frequency domain (referred to hence forth as the Fourier domain), and it assumes certain analogies between the Fourier domain and the spatial domain. It is now well established that representation of the spatial properties of visual stimuli in the Fourier domain is appropriate and that the locations of stimuli in that domain provide a satisfactory basis for describing both empirical and theoretical relationships among them (e.g. Shapley & Lennie, 1985; Olzak & Thomas, 1986; De Valois & De Valois, 1988; Wilson, Levi, Maffei, Rovamo, & De Valois, 1990). The validity of the assumed analogies between the Fourier domain and the spatial domain is less well established. However, it seems safe to assume, as we do, that the desensitizing influences of a stimulus spread to nearby stimuli in both domains. Further, there is evidence to support our assumption that the magnitude of the desensitization depends on both the luminance of the desensitizing stimulus (e.g. Whittle & Swanston, 1974) and the amplitude of the masking component (e.g. Legge & Foley, 1980).

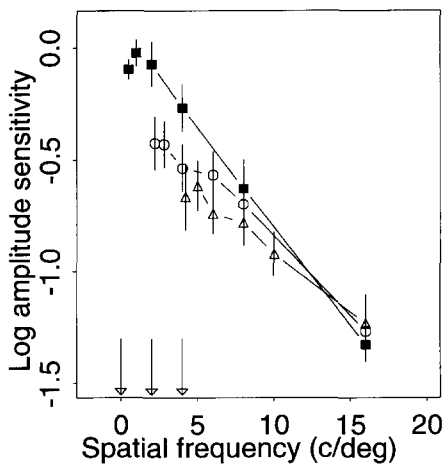

FIGURE 3. Same as Fig. 1, except that the temporal frequency of the test gratings was 4 Hz.

Operation in the spatial frequency domain

To establish a quantitative model of grating sensitivity in the presence of a masking stimulus, we first quantify the effects of the mask and the test components. The Fourier components of the luminance profile of a grating are shown in Fig. 4(a), with one component at zero frequency and the other at the frequency of modulation, f_L. As the signal enters and passes through the visual system, the effects of the two frequency components tend to spread, as illustrated in Fig. 4(b). There are a number of ways to think about this spread, but one metaphor that springs to mind is that of hypothetical channels (Graham, 1972). The sensitivity of a spatial frequency channel spreads beyond the frequency to which it is most sensitive; hence, a given Fourier component stimulates many channels with peak sensitivities spanning a range frequencies, but the excitation of a given channel decreases with its distance from the Fourier component in Fourier space. The height of the lightly shaded area in Fig. 4(b) can be taken to represent the strength of channel excitation by the d.c. component, and the location on the x-axis as representing the frequency at which the channels represented have peak sensitivity. The more darkly shaded area then would represent additional excitation by the test component at f_L. The model shown in Fig. 4 treats the zero frequency component like any other; so, in terms of channels, the model assumes that the channels with peak sensitivity to low spatial frequencies are somewhat excited by the zero frequency component.

Spatial inhomogeneity within the visual system also spreads excitation in the frequency domain. For example, sensitivity might decrease towards the periphery. Therefore the luminance distribution of a grating is attenuated by varying amounts in different parts of the visual field, and the Fourier spectrum of a grating after such attenuation spreads according to its convolution with the Fourier transform of the profile of attenuations.

In any case, as Fig. 4(b) shows, reducing the modulation of a grating to 0, so that the grating is reduced to a homogeneous field, does not entirely eliminate the

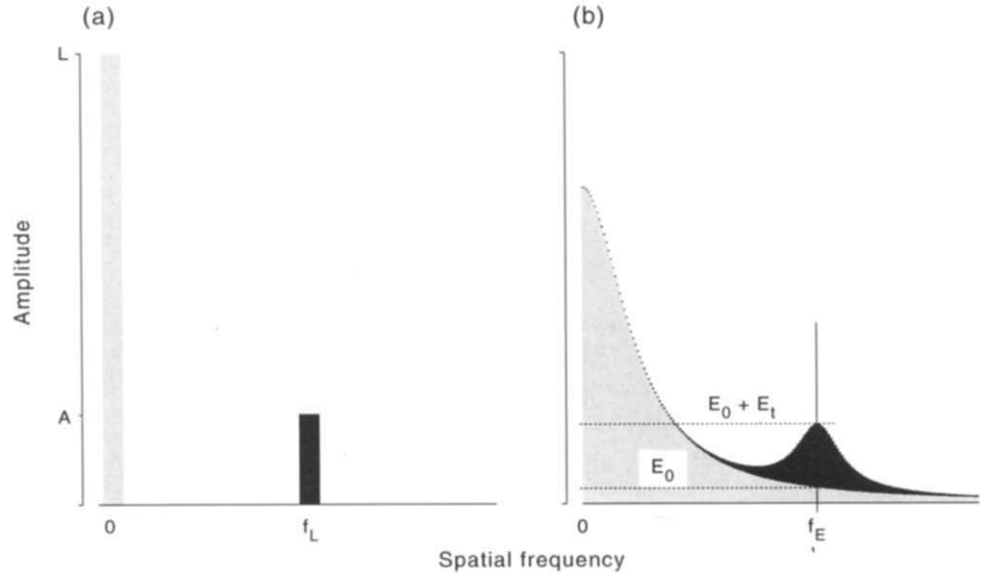

FIGURE 4. An illustration of the representation of a grating in the Fourier domain for: (a) a physical grating with spatial frequency, f_L; and (b) the representation of the grating after some visual processing; E_0 is the excitation at the frequency, f_E, spread from zero frequency, and E_t is the excitation at the frequency, f_E, spread from the component at the test frequency.

excitation at f_E, for some excitation spreads from 0 frequency to any given frequency, f_E. We denote that excitation, i.e. the excitation at any given frequency, f_E, in the absence of stimulus modulation, as E_0. Then we assume that threshold excitation, E_{th}, is reached when the difference between excitation by a test grating, E_t, and the excitation from other sources, such as that by the zero frequency component, E_0, and noise, N, satisfies some relationship:

$$E_{th} = tva(N, E_0). \tag{2}$$

The expression, *tva*, stands for threshold vs amplitude [it is shown below, in equation (3), that E_0 depends on amplitude], by analogy to the threshold vs intensity relationship in the spatial domain. Thus, the problem comes down to defining the function, $tva(N, E_0)$, and determining N and E_0.

Three-stage processing

Any model is a compromise between faithfulness of representation and tractability of the model; here we have chosen the three-stage model shown in Fig. 5. The first stage is a linear space-invariant filter that represents physical limits on the capacity of the visual system to pass information at high spatial frequencies; $M(f_L)$ is the modulation transfer function of the system, which includes losses caused by optics, receptors, and neural processing.

The second stage is also a linear filter, $G(f_E, f_L)$, but it provides for the effects of spatial inhomogeneity and represents the magnitude of excitation at frequency, f_E, that spreads from the input frequency, f_L, as discussed above.

The third stage is a nonlinear process, i.e. a threshold, whereby a response is generated if and only if the amplitude of the test grating, A_t, equals (or exceeds) the threshold determined by the *tva* function [equation (2)].

Then, the excitation by the zero frequency component, E_0, at any given spatial frequency, f_E, is

$$E_0(f_E) = \eta_0 A_0 M(0) G(f_E, 0), \tag{3}$$

where η_0 is a parameter that reflects the magnitude of excitation by the zero frequency component, $A_0 = L$ (the mean illuminance at the retina), $G(f_E, 0)$ is the spread function of the zero order term in the frequency domain,

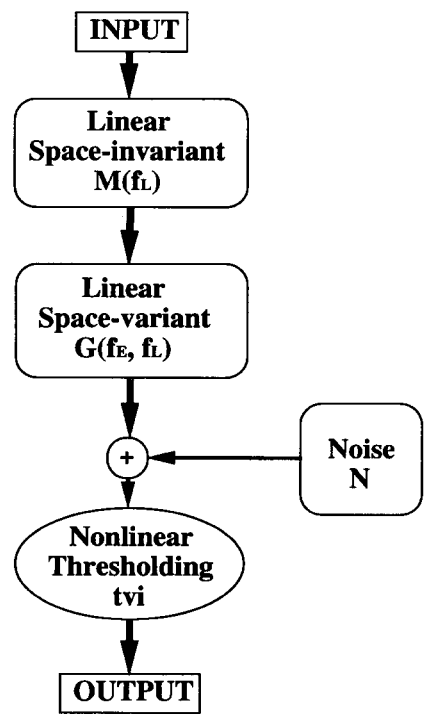

FIGURE 5. A three-stage model of visual processing: Linear space-invariant filter M, linear space-variant filter G, and nonlinear threshold described by the *tva* function. Noise enters between the second and third stage.

and $M(0)$ is the value of the linear space-invariant filter at zero spatial frequency ($f_L = 0$). The excitation by the test component, E_t, at any given spatial frequency, f_E, is:

$$E_t(f_E) = A_t M(f_{Lt}) G(f_E, f_{Lt}), \quad (4)$$

where the amplitude of the test component, $A_t = LC_t$; $M(f_{Lt})$ is the value of the linear space-invariant filter at the spatial frequency of the test grating, f_{Lt}; and $G(f_E, f_{Lt})$ is the function describing the spread of excitation from the test frequency in the frequency domain. The peak of the excitation described by equation (4) (illustrated in Fig. 4) determines the threshold amplitude of the test grating. As this model applies to narrow band sinusoidal stimuli, we assume that maximum excitation lies at the test frequency, where $f_E = f_{Lt}$.

Modulation transfer function

When the log of threshold contrast (or amplitude) is plotted against linear spatial frequency, the curve at relatively high spatial frequencies is close to a straight line with negative slope (Campbell, Kulikowski & Levinson, 1966), and this relationship holds true also for the curves in Figs 1–3. Therefore the relationship between threshold contrast and spatial frequency at high frequencies is exponential. At these high spatial frequencies the spread from the zero frequency component is low and has little effect. Hence, we assume that the contrast sensitivity curve at high spatial frequencies reflects the shape of the filter M, without contamination by the effects of the zero order term. Yang and Makous (1994a) have provided further support for that assumption. Thus, we assume:

$$M(f_L) = e^{-\alpha f_L}, \quad (5)$$

where α is a spatial frequency constant.

Frequency spread function

As discussed above, certain properties of the visual system would cause the Fourier spectrum of a stimulus to spread as its signal propagates through the system. We compared the suitability of Gaussian functions, exponential functions, and symmetric zero order Cauchy functions (Klein & Levi, 1985) to describe this spread of Fourier components in the Fourier domain. Empirically, the Cauchy function fits our data best. Thus we write:

$$G(f_E, f_L) = \frac{\sigma^2}{(f_E - f_L)^2 + \sigma^2}, \quad (6)$$

where σ is a parameter that determines the half width of the spread for a given grating frequency, f_L; this function is normalized, with unit value at $f_E = f_L$. Note that, as an exponential function is the Fourier transform of an Cauchy function, equation (6) is consistent with an exponential decline of excitation in the spatial domain.

Threshold vs amplitude relationship

Equation (2) calls for a function that relates the threshold amplitude of the test grating, E_{th}, to the amplitude of the zero frequency component in the Fourier domain, E_0. For this we adopted a function that has proven successful in the spatial domain (e.g. Chen & Makous, 1989):

$$E_{th} = tva = (N + E_0)^{\gamma}. \quad (7)$$

In this general form of the *tva* function, N is a parameter called noise for reasons described below. The parameter, γ, is the asymptotic slope in a log–log plot at high luminance.

The visual system is subject to an irreducible intrinsic noise, or *dark noise* (Barlow, 1956, 1957; Pelli, 1990; Makous, 1990), denoted here, N_0; and shot noise associated with the random absorption of photons, which increases in proportion to the square root of the luminance (deVries, 1943; Rose, 1948). The intrinsic noise determines the asymptote towards which threshold approaches as the excitation by light, E_0, approaches zero. Hence, the expression for noise must include at least these two components; i.e.:

$$N = N_0 + \beta L^{1/2}, \quad (8)$$

where, β is the coefficient of the luminance noise. As the noise here is independent of spatial frequency, it is a white noise. Thus N is proportional to the equivalent noise of the system. In the current model, it represents the amount of noise applied to the third stage (see Fig. 5).

The expression for the amplitude of any test grating is A_t, but the amplitude of a threshold test grating is denoted, A_{th}. Similarly, excitation by any test grating is E_t, but threshold excitation by the test grating is E_{th}. Combining equations (3), (4) and (7), shows that the amplitude of a test grating that is necessary for detection at a given frequency, f_E, is expressed by the ratio:

$$A_{th}(f_E) = \frac{(N + E_0)^{\gamma}}{M(f_{Lt}) G(f_E, f_{Lt})}.$$

If sensitivity is determined by the most strongly excited channel (i.e. the channel most sensitive under those conditions), the amplitude threshold, A_{th}, is determined by the minimum of the curve expressing amplitude as a function of spatial frequency. For sinusoidal stimuli, the frequency f_E at which the minimum occurs is close to but not exactly at the test frequency, f_{Lt}. To simplify the computations, we assume that the minimum is right at the frequency of the test grating, i.e. $f_E = f_{Lt}$, even though it actually lies at a slightly higher frequency. The error associated with this approximation is discussed below. Then, combining equations (2)–(8) yields an expression for the amplitude of a threshold grating:

$$A_{th} = e^{\alpha f_{Lt}} (N + E_0)^{\gamma}$$

$$= e^{\alpha f_{Lt}} \left(N_0 + \beta L^{1/2} + \frac{\eta_0 \sigma_0^2 L}{f_E^2 + \sigma_0^2} \right)^{\gamma}, \quad \text{for } f_E = f_{Lt}, \quad (9)$$

with six undetermined parameters. η_0 is a parameter that scales the magnitude of masking by the zero frequency component. For example, if the background differs from the test component along dimensions other than spatial

frequency, such as color or temporal frequency, masking strength, η_0, might be expected to diminish.

Masking grating

When the stimulus includes a masking frequency other than the zero frequency component, excitation at any given frequency, f_E, includes one more term, which we define as E_m, the excitation produced by a masking grating:

$$E_m(f_E) = \eta_m A_m M(f_{Lm}) G(f_E, f_{Lm}), \quad (10)$$

where $A_m = LC_m$ (the amplitude of the masking component); $G(f_E, f_{Lm})$ is the spread of the mask frequency, f_{Lm}, to any other given frequency, f_E; and η_m is a parameter that scales the magnitude of masking.

The term A_m, then, is an additional source of excitation at the frequency, f_F. This has two consequences: first, it raises thresholds approximately in proportion to the the excitation it produces at the test frequency; but when the masking grating is itself below threshold, the excitation it produces at the test frequency sums with that of the test grating to reach threshold (Yang & Makous, 1995; Makous & Yang, in preparation). Thus, the amplitude threshold of the test is given by (Yang & Makous, 1995):

$$A_{th} = e^{\alpha f_{Lt}}(N + E_0 + E_m)^{\gamma} - \rho G(f_{Lt}, f_{Lm}). \quad (11)$$

Here E_m represents the contribution to excitation by the masking grating, and the last term accounts for subthreshold summation. The factor, $G(f_{Lt}, f_{Lm})$, reflects the fact that subthreshold summation diminishes as the difference between the frequencies increases (its form is identical to equation (6) with f_{Lt} in place of E and f_{Lm} in place of L), and:

$$\rho = A_m G(f_{Lt}, f_{Lm}) \frac{A^{*2}}{[A_m G(f_{Lt}, f_{Lm})]^2 + A^{*2}}. \quad (12)$$

Equation (12) has three effects: when the masking grating is below threshold itself, a threshold response depends on the sum of the masking grating and the test grating; when the pedestal is well above threshold, the term in equation (12) tends towards zero, and threshold depends on the tvi function in equation (11); and equation (12) allows for a gradual transition from conditions where the masking grating is below threshold to those where it is above threshold. The assumption of subthreshold summation is based on unpublished observations and on the data of Yang and Makous (1995), and it fits the present data adequately except that in its simplest form, it requires the threshold amplitude of the test grating to reach a minimum value of zero. The variability of thresholds, and possibility other sources of variability in the nervous system, may prevent observation of this ideal value. The deviation from this ideal could probably be modeled by introducing at least one more source of random variability in the model, but that would require fitting at least two additional free parameters; instead we use the expression in equation (12) because it adequately describes the data without any free parameters, even though it has no theoretical basis.

According to equation (12), then, to arrive at the threshold amplitude for the test grating, one must subtract the contribution by the masking grating, A_m, after the difference between the frequencies of mask and test gratings has been taken into account. If the two frequencies are the same, as in a pedestal experiment, $G(f_{Lt}, f_{Lm})$ drops out, leaving only A_m and A^*, and the equation is identical to equation (8) in Yang and Makous (1995). A^* is the amplitude threshold determined by equation (9).

Then threshold is reached when a test grating raises the excitation above that caused by all other sources of excitation—masking grating, zero frequency masking and noise—by an amount specified in the *tva* function expressed by equation (11).

Model fits

In the experiments, we measured the contrast sensitivities with the three observers at four luminance levels, as mentioned above. The results for the individual observers are shown by the data points in Figs 6–8. Error bars represent ± one standard error of the mean. Where no error bar is visible, it is smaller than the symbol.

In the model, L is the mean retinal illuminance, which is the product of the mean luminance L^* and pupil area. To compare zero frequency masking with masking at other frequencies, which was our primary purpose, it was not necessary to control pupil size. However, to measure the effects of luminance quantitatively, it is necessary to know the retinal illuminance; to do so, we photographed the eyes of the observers under the conditions used in the experiments, and measured the pupil diameters, which are shown in Table 1.

We used a nonlinear, least-square program (part of Splus, in the Unix operating system) to optimize the free parameters to fit the experimental data. However, in the course of fitting we found that the values of σ for the two non-zero masking components were the same, and also that:

$$\eta_m = \eta f_{Lm}^{1/2}, \quad (13)$$

for the two frequencies we used for masking gratings. The unsubscripted constant, *eta*, is a free parameter of proportionality.

This leaves equation (11) with one set of eight free parameters to describe 12 curves for each observer, less than one parameter per curve. The smooth curves in Figs 6–8 are the results of fitting equation (11) to the data. The eight best-fitting parameters for the three observers are shown in Table 2.

The most noticeable systematic deviation of the model from the data is in the slopes at the lower luminances, which tend to be too shallow. This tendency is obvious in the data of all the three observers. This may follow from the fact that we used the same filter, M, for all luminances. One might expect the slope of M to get steeper when the luminance decreases, owing to an increase of the summation area with luminance (e.g. Barlow, 1958) and the tendency toward lower optical

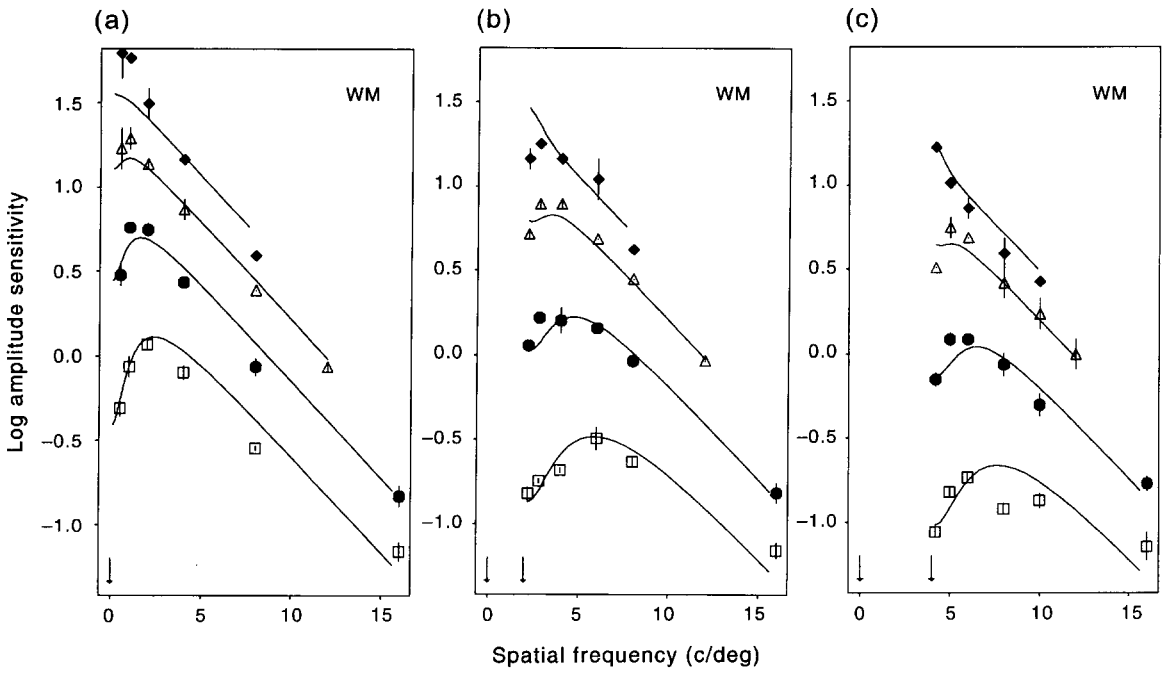

FIGURE 6. Amplitude sensitivities at four luminance levels: 25 (□), 2.1 (●), 0.20 (△), and 0.019 (◆) cd/m^2 for observer WM. (a) The detection sensitivity curves. (b, c) The masked sensitivity curves with mask spatial frequency at 2 and 4 c/deg, respectively. The error bars represent the standard errors over four repetitions. The arrows point to the mask frequencies, including zero as a masking frequency. The smooth curves are the optimal fits of equation (11).

quality of the eye (Campbell & Gubisch, 1966) as the pupil size increases with decreasing luminance (see Table 1).

Data from the literature

Here we push on to see whether the current model can handle other contrast sensitivity data in the literature. The model expressed by equation (11) can be used to calculate detection threshold with or without a masking grating. In the conventional enterprise of measuring contrast sensitivity functions, the test grating contains only the test frequency and zero frequency components; that is, the masking component amplitude $A_m = 0$. In this case, equation (11) collapses to the form of equation (9).

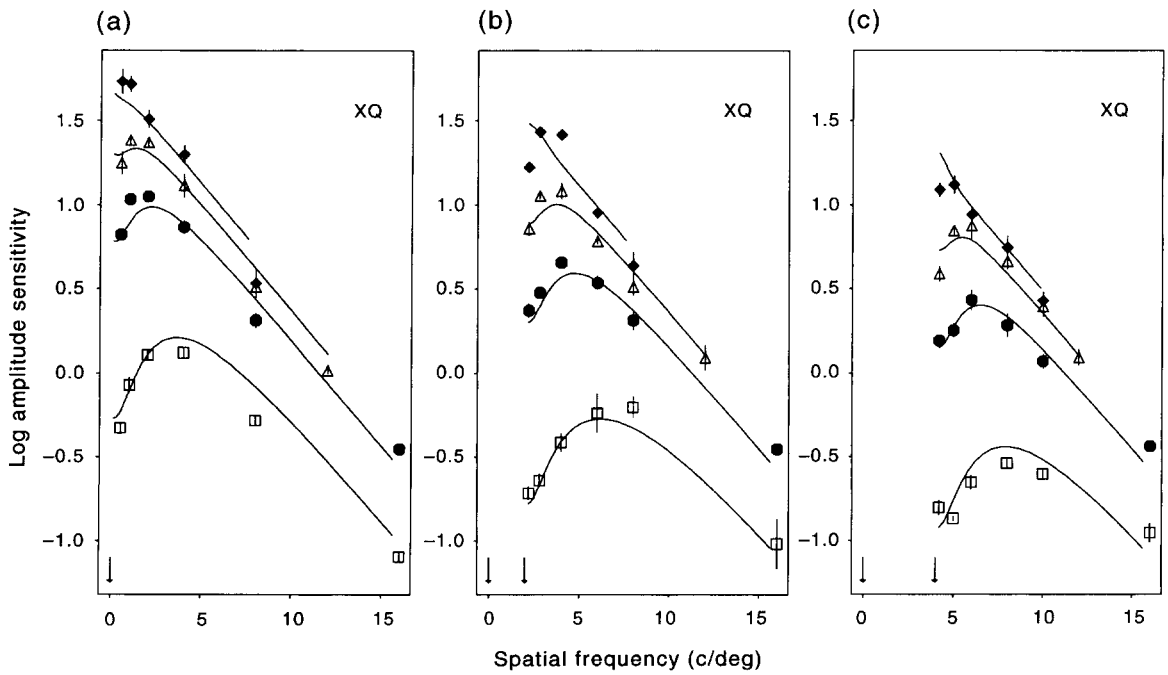

FIGURE 7. Amplitude sensitivities at four luminance levels: 42 (□); 2.1 (●); 0.20 (△); and 0.019 (◆) cd/m^2 for observer XQ. Otherwise, the same as Fig. 6.

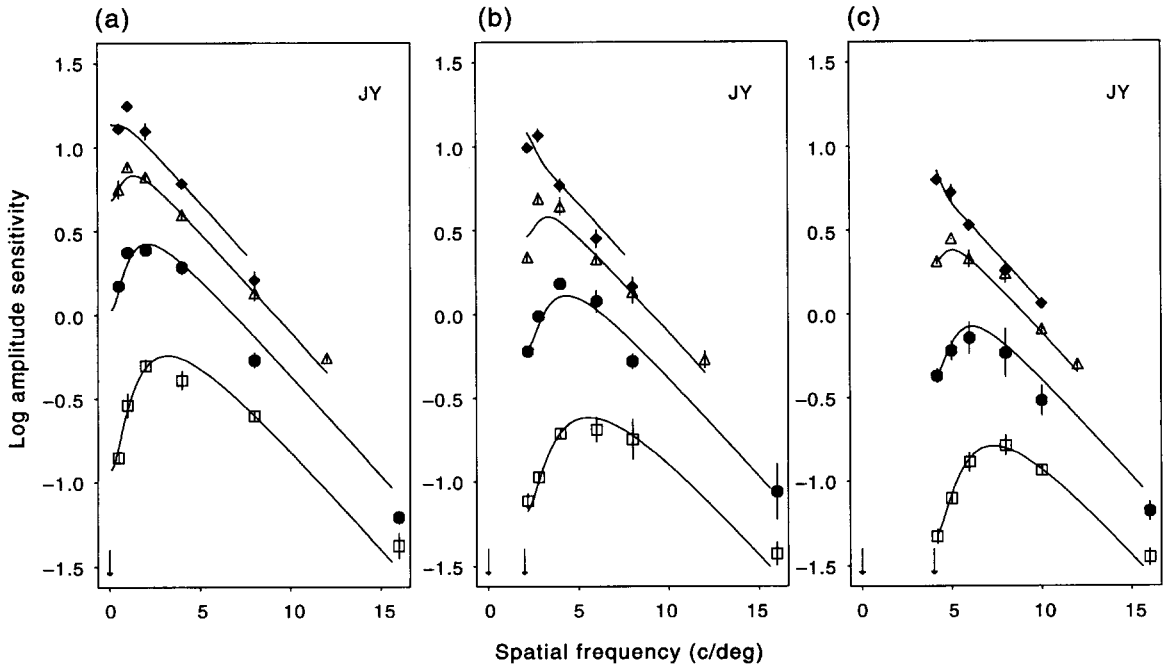

FIGURE 8. Same as Fig. 7, for observer JY.

The data points in Fig. 9 are those of Van Nes and Bouman (1967), obtained at mean luminances ranging over seven log units; however, we have replotted the curves with amplitudes in place of contrasts. The smooth curves show the fits of equation (9), and the sets of six free parameters required to fit the set of seven curves are listed in Table 2.

The fit is roughly comparable to those of the data from the present study. As in Figs 6–8, the largest deviations tend to come from the data at the lowest luminance levels, where the actual modulation transfer function might be steeper than the fits.

Figure 10 shows analogous data obtained by Kelly (1972), along with the theoretical fits of equation (9). The corresponding values of the six parameters are shown in Table 2.

The essence of these data are reasonably captured by the theory, with some local inaccuracy. From one point of view, the fact that six free parameters were sufficient to fit seven curves (Fig. 9) is satisfactory. In this sense, the model provides an economical way to describe the experimental data, for the information in the 108 data points in Fig. 9, or the information of the 44 points in Fig. 10, is reduced to a set of six numbers.

TABLE 1. The pupil diameters (in mm) of the three observers at different mean luminances

	Mean luminance (cd/m^2)				
Observer	42	25	2.1	0.20	0.019
WM		3.6	4.0	4.5	5.2
XQ	3.3		3.6	5.0	6.2
JY	4.8		6.0	7.3	8.5

DISCUSSION

Masking by the zero frequency component

We have satisfactorily treated contrast sensitivity curves as though they were subject to masking by the zero frequency component of the test gratings, and such masking is qualitatively analogous to the masking by a grating in every way so far tested. This, however, does not prove that the processes are the same. For one thing, there are quantitative differences between the two kinds of masking. For example, the spread parameter for the 0 frequency component (σ_0) differs from those of the 2 and 4 c/deg components, which were identical to one another (σ_m); and the relationship between amplitude of the 0 frequency masking component and the strength of masking (η_0) differs from that between the modulation amplitude and the strength of masking (η_m), a difference that increases with spatial frequency [cf. equation (13)].

Aside from the quantitative differences, the present observations also do not distinguish between the effects

TABLE 2. The parameters obtained by optimizing the fits of the model to the experimental data. Source codes: WM, XQ and JY are the data from the three observers of the present experiments (see Figs 6–8); VB represents the data of Van Nes and Bouman (1967) (see Fig. 9), and Kelly represents the data of Kelly (1972) (see Fig. 10)

	Parameter							
Source	α	β	γ	N_0	η_0	σ_0	η	σ_m
WM	0.26	0.016	0.95	0.0092	0.0094	0.58	0.19	1.18
XQ	0.29	0.003	0.91	0.0093	0.0052	0.93	0.12	0.95
JY	0.28	0.011	0.91	0.027	0.0133	0.61	0.16	0.76
VB	0.12	0.012	1.15	0.0003	0.0090	1.10		
Kelly	0.43	0.004	0.97	0.0000	1.25	0.04		

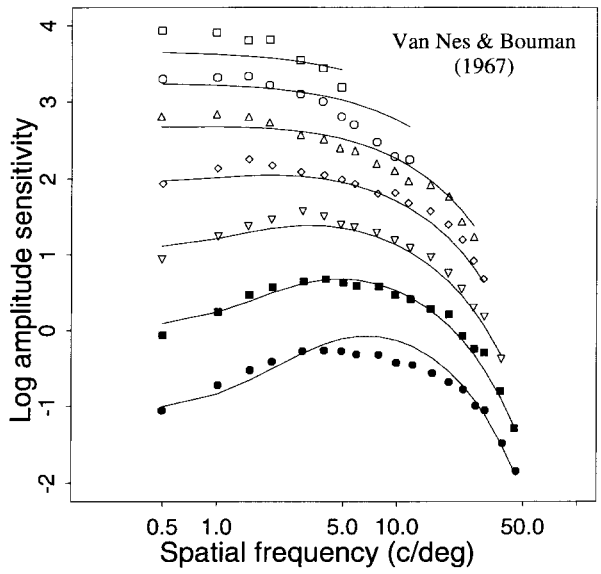

FIGURE 9. Data of Van Nes and Bouman (1967) at seven retinal illuminances, 0.0009–900 td, increasing in steps of one log unit from top down. The smooth curves are the optimal fits of equation (9) with a single set of six parameters (see Table 2).

of low-frequency noise (Pelli, 1990), and other causes of desensitization such as are more likely to account for masking by gratings. Visual noise and the zero frequency component are alike in that they are both present in the test stimulus, and they both raise thresholds. In equation (9), threshold amplitude, A_{th}, can be increased either by noise (N) or by the zero frequency component (last term within the parentheses), so the effect of the zero frequency masking is equivalent to adding noise to the system. The combined effect, or equivalent noise, is simply:

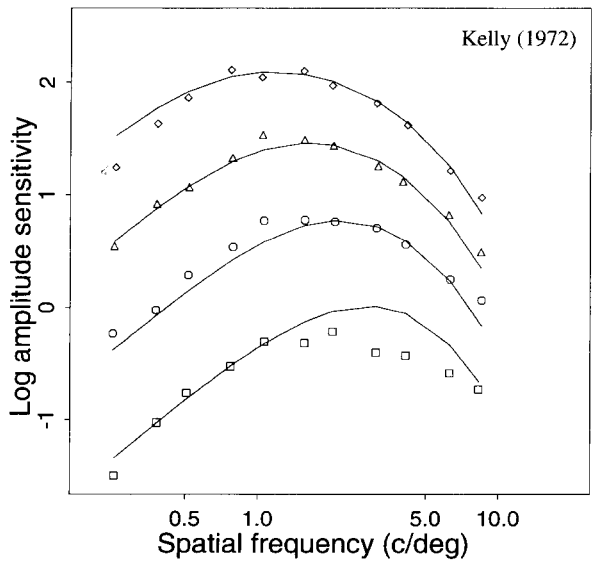

FIGURE 10. Data of Kelly (1972) at four retinal illumination levels, 0.72, 7.2, 72, and 720 td (from top down). The smooth curves are the optimal fits of equation (9) with a single set of six parameters (see Table 2).

$$N_{eq} = N_0 + \beta L^{1/2} + \frac{\eta_0 \sigma_0^2 L}{f^2 + \sigma_0^2}, \tag{14}$$

from equation (9).

At fixed illuminance (L), the first two terms of the equivalent noise are constant, and the last term decays rapidly with spatial frequency, so the whole equivalent noise peaks at zero frequency and flattens at high frequencies. This is in agreement with the noise surface reported by Pelli (1990) in the spatiotemporal frequency domain: Pelli (1990) attributes the flat part to the shot noise of photons, and the part that rises at low frequencies to neural noise, which may be indistinguishable from masking.

Another potential problem in attributing the masking by the 0 frequency component to the processes that account for grating masking is that evidence of the required low frequency channels is scarce (e.g. Legge, 1979; Wilson, McFarlane & Phillips, 1983). However, this may simply be the consequence of the very masking hypothesized. In other words, masking of the very low frequency channels by the zero frequency term would tend to conceal their existence. Indeed, Stromeyer, Klein, Dawson and Spillmann (1982) revealed the existence of very low spatial frequency channels by adapting with dynamic noise or temporally modulated gratings.

Relations to visual properties

The model derived here by treating the zero frequency component as a masking stimulus explains the malleability of the contrast sensitivity curve observed in the presence of other gratings, and it gracefully incorporates changes under varying levels of illumination. It is worth pointing out that the model is faithful to the classical finding that Weber's law holds at low spatial frequencies, and the deVries–Rose law holds at high spatial frequencies (e.g. Van Nes & Bouman, 1967; Kelly, 1972). When spatial frequency is low, sensitivity is dominated by masking by the zero frequency term, which grows linearly with mean luminance, and the noise terms can be neglected, so that:

$$A_{th} = e^{\alpha f}\left(\eta_0 \sigma_0^2 \frac{L}{f^2 + \sigma_0^2}\right)^{\gamma}, \tag{15}$$

which is close to Weber's law if γ is close to unity, as it is. However, if spatial frequency is high, masking by the zero frequency component can be neglected, so that:

$$A_{th} = e^{\alpha f}(\beta L^{1/2})^{\gamma}, \tag{16}$$

which is close to the deVries–Rose law.

In this paper we used analytical functions to capture the general trends in the data without worrying too much about local details. At a minimum, the model economically describes contrast sensitivity under a variety of conditions. However, it also provides cues to underlying mechanisms and the interplay of variables in determining visual sensitivity. For example, the value of α gives the approximate modulation transfer function of the entire system, and γ represents the asymptotic slope of the *tva* function on log–log axes. As the γ values are

close to unity (see Table 2), Weber's law is guaranteed at high background levels, and for many purposes γ can be set at unity, which makes the model more tractable and reduces the number of free parameters. The value of N_0 provides an estimate of the absolute intrinsic noise, and β the increase of noise with increasing retinal illuminance. The most surprising result is that the masking strength increases with spatial frequency, and this warrants further study.

Note that this three-stage model could be expressed as a two-stage model consisting of a linear filter followed by a nonlinear *tva* mechanism. However, the extra stage allows separate treatment and examination of the effects on visual sensitivity caused by physical inhomogeneities in the stimuli and in the visual system.

Limitations of the model

Naturally, it is hard to establish how well the model derived here can be extrapolated to conditions not tested. The fit to studies (Figs 9 and 10), performed under greatly different conditions is encouraging.

Less encouraging is the variation among some of the estimated parameters. Several of these trade-off against one another, and as a consequence wide variations in one can be compensated by similarly wide variations in another so as to achieve small gains in goodness of fit. This, compounded by the complexity of the model, has prevented us from establishing meaningful fiducial limits on these parameters. Thus, at this stage, we do not know which of these differences are meaningful and which are within the error of estimation. Until this problem is better understood, the value of the model for estimating fundamental parameters of the visual system is in some respects limited. A separate unanswered question relating to the generality and usefulness of the model is how well it applies to stimuli with many masking components, such are typical of the conditions under which the visual system normally operates.

The main focus of this paper is on the conventional contrast sensitivity curve. According to the concept of zero frequency masking, the conventional contrast sensitivity curve reflects the effects of masking of test frequencies near the component that all visual stimuli have at 0 c/deg. In this particular case, all physically realizable stimuli lie above the masking frequency. Hence, it is appropriate to compare zero frequency masking only with the masking of test frequencies *above* other masking frequencies, and that is what we have done here. Data points below the masking frequency are not relevant for present purposes. However, it is important to point out that we have not tested frequencies below the masking frequency in these experiments, and they are not covered by the model. There is no reason to suppose that the masking function is symmetrical, and preliminary data suggest that it is not.

Here, we estimate the error caused by assuming that maximum excitation is at the spatial frequency of the test grating, i.e. $f_E = f_{Lt}$ (cf. Fig. 4). With the parameters for JY shown in Table 2, the largest error occurs at the lowest spatial frequency (0.5 c/deg) and the highest luminance (42 cd/m^2), where the threshold without the approximation would be 0.1 log unit lower than that given by equation (9); and the threshold at 1 c/deg, at the same luminance, is 0.05 log unit lower. The data of the other observers yield similar values. As the curves fit the data better than is consistent even with a small error of this size, the curve fitting process compensates for the effects of this error of approximation and introduces a corresponding error in the fitted parameters. However, this error affects only a few of the many observations that determine the estimated value of the parameters, and the associated error is likely to be small relative to other sources of error.

Comparison of models

Low frequency attenuation. Aside from the present theory of zero frequency attenuation, attenuation of sensitivity to low spatial frequencies has previously been attributed to such mechanisms as frequency selective channels (e.g. Wilson, *et al.*, 1983; Foley & Yang, 1991; Hess & Snowden, 1992), neural lateral inhibition (e.g. Kelly, 1975), and frequency dependent spatial summation (Hoekstra, van der Goot, van den Brink & Bilsen, 1974; Estevez & Cavonius, 1976; Banks, Geisler & Bennett, 1987; Sekiguchi, Williams & Brainard, 1993). Present evidence does not establish which is true, but it is possible to sort out some of their strengths and weaknesses.

Conventional channel theory concerns mainly the number of channels and their shape, and attributes the insensitivity of the visual system at low frequencies to a lack of channels sensitive to these low frequencies. Such theories are embarrassed by a superabundance of free parameters, as four parameters are typically required to describe each channel (cf. for example, the popular difference-of-Gaussian model). Furthermore, as Snowden, Waugh and Hess (1993) have shown in the temporal domain, these parameters may well have to vary with mean luminance to fit the experimental data. This compounds the problems of channel specification.

Lateral inhibition has an established physiological basis (Derrington & Lennie, 1982; Enroth-Cugell, Robson, Schweitzer-Tong & Watson, 1983) and has been used to model human visual sensitivity (Rohaly & Buchsbaum, 1989). However, the absence of an established relationship between the receptive fields of the model and the receptive fields observed physiologically deprives the theory of much of its physiological support. More important, the band-pass spatial contrast sensitivity function observed at high temporal frequencies when in-phase modulation is used (Yang & Makous, 1994a) is difficult to reconcile with an explanation of the low frequency attenuation that is based on lateral inhibition. When counterphase modulation is high in temporal frequency, the attenuation at low spatial frequencies disappears. The physiologically based explanation is that the center and the surrounds come into synergy owing to a delay affecting the signals from the

surround mechanisms. But in-phase modulation at high temporal frequencies shows no diminution of the low frequency roll-off. The explanation of the results of counter-phase modulation should apply also to in-phase modulation, but the consequences of the assumed phase delay are absent.

The theory based on summation area is inferred primarily from the effects of stimulus area on sensitivity to different frequencies (Savoy & McCann, 1975; Howell & Hess, 1978; Robson & Graham, 1981). This inference is plausible enough, but it does not exclude alternatives, and it has no more physiological basis than zero frequency masking. A quantitative model of sensitivity to low frequency gratings has been developed by Rovamo, Luntinen and Näsänen (1993) on the basis of this theory, but the range of conditions to which the theory applies is limited. The more recent work by Rovamo, Mustonen and Näsänen (1994), based on the additional assumptions of a low-pass optical filter, a high-pass neural filter, and internal neural noise, is much more powerful and is applicable to contrast sensitivity curves of varying luminance and field size. However, this model does not easily handle changes in the contrast sensitivity function with changes in other variables, such as temporal frequency; and the assumption that the neural filter is high-pass, and therefore cannot pass information in very low spatial frequencies, is probably false (Yang & Makous, 1994b).

The chief advantages of the theory based on zero frequency masking lie in its descriptive power and in its foundation on concepts that, for the most part, relate in plausible ways to classically recognized constraints on visual sensitivity. Its chief drawbacks may be a want of obvious physiological mechanisms for zero frequency masking and difficulty in relating the concept to the results of experiments conceived and interpreted in the spatial domain. However, difficulty in relating psychophysics to physiology are hardly peculiar to the present theory. From the physiological perspective, the principal problem, is separating retinal from cortical effects and separating low frequency masking from what has been called lateral inhibition. Although a cortical contribution might seem to be excluded by the unresponsiveness of cortical neurons to flashed uniform fields, information on the mean luminance in many neurons of the waking striate cortex may lie in their tonic activity (Kayama, Riso, Bartlett, & Doty, 1979). As for the spatial domain, the spread of desensitization that can be expressed either in the Fourier or the spatial domain. The spread parameter of 0.5–1 c/deg in the Fourier domain corresponds to a corresponding space constant for the spread of desensitization of 6–12 deg This is larger than has typically been observed in spot-and-flash experiments. Highly local adaptation (Cicerone, Hayhoe, & MacLeod, 1990; Burr, Ross, & Morrone, 1985), however, would not show up as a frequency-specific effect in experiments such as these that go no higher than 16 c/deg.

Until more evidence accumulates, these theories may have to be judged chiefly on their utility and their coherence with related experiments.

Masking vs adaptation. It has been suggested that the main functional difference between masking and adaptation is that masking can facilitate detection but adaptation never does (e.g. Ross & Speed, 1991; Foley & Yang, 1991). This facilitation is often regarded as the outcome of dis-inhibition between different frequency selective channels. The inhibitory input is the most important component in the Foley's model (1994), for example. Many of models of masking assume a nonlinear transduction of contrast; then masking is proportional to the space derivative of this transducer function (e.g. Legge & Foley, 1980; Ross & Speed, 1991; Foley, 1994).

We prefer the alternative explanation of facilitation, which attributes facilitation to subthreshold summation (Kulikowski, 1976) for reasons that are explained elsewhere (Yang & Makous, 1995). This cleaves facilitation from masking as a separate phenomenon. Those of us who adopt the subthreshold summation hypothesis and would yet preserve the distinction between masking and adaptation must therefore look for an alternative basis for the distinction.

REFERENCES

Banks, M. S., Geisler, W. S. & Bennett, P. J. (1987). The physical limits of grating visibility. *Vision Research, 27*, 1915–1924.

Barlow, H. B. (1956). Retinal noise and absolute threshold. *Journal of Optical Society of America, 46*, 634–639.

Barlow, H. B. (1957). Increment thresholds at low intensities considered as signal/noise discriminations. *Journal of Physiology, London, 136*, 469–488.

Barlow, H. B. (1958). Temporal and spatial summation in human vision at different background intensities. *Journal of Physiology, London, 141*, 337 350.

Burr, D. C., Ross, J. & Morrone, M. C. (1985). Local regulation of luminance gain. *Vision Research, 25*, 717–727.

Campbell, F. W. & Gubisch, R. W. (1966). Optical quality of the human eye. *Journal of Physiology, London, 186*, 558–578.

Campbell, F. W., Kulikowski, J. J. & Levinson, J. (1966). The effect of orientation on the visual resolution of ratings. *Journal of Physiology, London, 187*, 427–436.

Chen, B. & Makous, W. (1989). Light capture by human cones. *Journal of Physiology, London, 414*, 89–109.

Cicerone, C. M., Hayhoe, M. M. & MacLeod, D. I. A. (1990). The spread of adaptation in human foveal and parafoveal cone vision, *Vision Research, 30*, 1603–1615.

Derrington, A. M. & Lennie, P. (1982). The influence of temporal frequency and adaptation level on receptive field organization of retinal ganglion cells in cat. *Journal of Physiology, London, 333*, 343–366.

De Valois, R. L. & De Valois, K. K. (1988). *Spatial vision*. New York: Oxford Univ. Press.

De Valois, R. L., Morgan, H. & Snodderly, D. M. (1974). Psychophysical studies of monkey vision—III. Spatial luminance contrast sensitivity tests of macaque and human observers. *Vision Research, 14*, 75–81.

deVries, H. L. (1943). The quantum character of light and its bearing upon threshold of vision, the differential sensitivity and visual acuity of the eye. *Physica, 10*, 553–564.

Enroth-Cugell, C., Robson, J. G., Schweitzer-Tong, D. E. & Watson, A. B. (1983). Spatio-temporal interactions in cat retinal ganglion cells showing linear spatial summation. *Journal of Physiology, London, 341*, 279–307.

Estevez, O. & Cavonius, C. R. (1976). Low-frequency attenuation in the detection of gratings: Sorting out artefacts. *Vision Research, 16*, 497–500.

Foley, J. M. (1994). Human luminance pattern-vision mechanisms: masking experiments require a new model. *Journal of the Optical Society of America A, 11*, 1710–1719.

Foley, J. M. & Yang, Y. (1991). Forward pattern masking: Effects of spatial frequency and contrast. *Journal of the Optical Society of America A, 8*, 2026–2037.

Graham, N. (1972). Spatial frequency channels in the human visual system: Effects of luminance and pattern drift rate. *Vision Research, 12*, 53–68.

Hess, R. F. & Snowden, R. J. (1992). Temporal properties of human visual filters: Number, shapes and spatial covariation. *Vision Research, 32*, 47–59.

Hoekstra, J., van der Goot, D. P. J., van den Brink, G. & Bilsen, F. A. (1974). The influence of the number of cycles upon the visual contrast threshold for spatial sine wave patterns. *Vision Research, 14*, 365–368.

Howell, E. R. & Hess, R. F. (1978). The functional area for summation to threshold for sinusoidal gratings. *Vision Research, 18*, 369–374.

Kayama, Y., Riso, R. R., Bartlet, J. R. & Doty, R. W. (1979). Luxotonic responses of units in macaque striate cortex. *Journal of Neurophysiology, 42*, 1495-1517.

Kelly, D. H. (1972). Adaptation effects on spatio-temporal sine-wave thresholds. *Vision Research, 12*, 89–101.

Kelly, D. H. (1975). Spatial frequency selectivity in the retina. *Vision Research, 15*, 665–672.

Klein, S. A. & Levi, D. M. (1985). Hyperacuity thresholds of 1 sec: Theoretical predictions and empirical validation. *Journal of the Optical Society of America A, 2*, 1170–1190.

Kulikowski, J. J. (1971). Some stimulus parameters affecting spatial and temporal resolution of human vision. *Vision Research, 11*, 83–93.

Kulikowski, J. J. (1976). Effective contrast constancy and linearity of contrast sensation. *Vision Research, 16*, 1419–1431.

Legge, G. E. (1979). Spatial frequency masking in human vision: Binocular interactions. *Journal of the Optical Society of America, 69*, 838–847.

Legge, G. E. & Foley, J. M. (1980). Conrast masking in human vision. *Journal of the Optical Society of America, 70*, 1458–1471.

Makous, W. (1990). Absolute sensitivity. In Hess, R. F., Sharpe, L. T. & Nordby, K. (Eds), *Night vision* (pp. 146–176). New York: Cambridge Univ. Press.

Olzak, L. A. & Thomas, J. P. (1986). Seeing spatial patterns. In Boff, K. R., Kaufman, L. & Thomas, J. P. (Eds). *Handbook of perception and human performance, Vol. 1, sensory processes and perception, Chapter 7.* NewYork: Wiley.

Pelli, D. G. (1990). The quantum efficiency of vision. In Blakemore, C. (Ed). *Vision: Coding and efficiency* (pp. 3—24). Cambridge: Cambridge Univ. Press.

Robson, J. (1966). Spatial and temporal contrast-sensitivity functions of the visual system. *Journal of the Optical Society of America, 56*, 1141–1142.

Robson, J. & Graham, N. (1981). Probability summation and regional variation in contrast sensitivity across the visual field. *Vision Research, 21*, 409–418.

Rohaly, A. M. & Buchsbaum, G. (1989). Global spatiochromatic mechanism accounting for luminance variations in contrast sensitivity functions. *Journal of the Optical Society of America A, 6*, 312–317.

Rose, A. (1948). The sensitivity performance of the human eye on absolute scale. *Journal of the Optical Society of America, 38*, 196–208.

Ross, J. & Speed, H. D. (1991). Contrast adaptation and contrast masking in human vision. *Proceedings of the Royal Society of London B, 246*, 61–69.

Rovamo, J., Luntinen, O. & Näsänen, R. (1993). Modelling the dependence of contrast sensitivity on grating area and spatial frequency. *Vision Research, 33*, 2773–2788.

Rovamo, J., Mustonen, J. & Näsänen, R. (1994). Modelling contrast sensitivity as a function of retinal illuminance and grating area. *Vision Research, 34*, 1301–1314.

Savoy, R. L. & McCann, J. J. (1975). Visibility of low-spatial-frequency sine-wave targets: Dependence on number of cycles. *Journal of the Optical Society of America, 65*, 343–350.

Sekiguchi, N., Williams, D. R. & Brainard, D. H. (1993). Efficiency in detection of isoluminant and isochromatic interference fringes. *Journal of the Optical Society of America A, 10*, 2118–2133.

Shapley, R. & Lennie, P. (1985). Spatial frequency analysis in the visual system. *Annual Review of Neuroscience, 8*, 547–583.

Snowden, R. J., Waugh, S. J. & Hess, R. F. (1993). Temporal frequency channels as revealed by masking at low luminance levels. *Investigative Ophthalmology & Visual Science (Suppl.), 34*, 706.

Stromeyer, C. F., III, Klein, S., Dawson, B. M. & Spillmann, L. (1982). Low spatial-frequency channels in human vision: Adaptation and masking. *Vision Research, 22*, 225–233.

Van Nes, F. L. & Bouman, M. A. (1967). Spatial modulation transfer in the human eye. *Journal of the Optical Society of America, 57*, 401–406.

Watson, A. B. & Pelli, D. G. (1983). QUEST: A Bayesian adaptive psychometric method. *Perception and Psychophysics, 33*, 113–120.

Whittle, P. & Swanston, M. T. (1974). Luminance discrimination of separated flashes: The effect of background luminance and the shapes of t. v. i. curves. *Vision Research, 14*, 713–719.

Wilson, H. R., Levi, D., Maffei, L., Rovamo, J. & De Valois, R. (1990). The perception of form: Retina to striate cortex. In Spillmann, L. & Werner, J. S. (Eds.) *Visual perception: The neurophysiological foundations* (Chapter 10). New York: Academic Press.

Wilson, H. R., McFarlane, D. K. & Phillips, G. C. (1983). Spatial frequency tuning of orientation selective units estimated by oblique masking. *Vision Research, 23*, 873–882.

Yang, J. & Makous, W. (1994a). Spatiotemporal separability in contrast sensitivity. *Vision Research, 34*, 2569–2576.

Yang, J. & Makous, W. (1994b). Sensitivity to sine- and cosine-wave gratings of low spatial frequency. *1994 OSA Annual Meeting/ILS-X Program*, 48.

Yang, J. & Makous, W. (1995) Modeling pedestal experiments with amplitude instead of contrast. *Vision Research, 35*, 1979–1989.

Acknowledgements—This research was supported by U.S. Public Health Service grants EY-4885 and EY-1319. We thank W. S. Geisler for his helpful suggestions.

APPENDIX

Physical Variables

x, y, t = 2-D space and time coordinates
s = luminance distribution of the visual stimulus
f_L = spatial frequency of luminance modulation
L^* = mean luminance
L = mean illuminance at the retina
f_{Lt} = spatial frequency of the test grating
f_{Lm} = spatial frequency of the masking grating
C_t = contrast of the test grating
C_m = contrast of the masking grating
A_0 = amplitude of the zero frequency component (equal to L)
A_t = amplitude of the test grating (equal to LC_t)
A_{th} = threshold amplitude of the test grating
A^* = threshold amplitude of the test grating with no mask
A_m = amplitude of the masking grating (equal to LC_m)
ω = temporal frequency of the testing grating modulation
ϵ = spatial phase of the grating (random)

Model Variables

f_E = spatial frequency coordinate of excitation in the visual system

M = modulation transfer function
G = frequency spread function
E_t = excitation by the test component
E_{th} = excitation by a threshold test component
E_0 = excitation by the zero frequency component
E_m = excitation by the masking component
N = noise applied at the detection stage
N_{eq} = equivalent noise
ρ = subthreshold summation of the mask with test grating

Free Parameters

α = frequency constant of the modulation transfer function
β = coefficient of the square-root noise
γ = asymptotic slope of log threshold vs log mask amplitude
σ_0 = half width of zero frequency spread
σ_m = half width of frequency spread for 2 and 4 c/deg gratings
η_0 = strength of zero frequency masking
η = strength of modulation frequency masking
N_0 = intrinsic noise